Tikrit Journal of Engineering Sciences (2025); 32(1): 1112
DOI: http://doi.org/10.25130/tjes.32.1.12

IRAQI Academic Scientific Journals

ISSN: 1813-162X (Print); 2312-7589 (Online)
Tikrit Journal of Engineering Sciences
available online at: http://www.tj-es.com

TJES Tikrit Journal of Engineering Sciences

Evaluating the Predicted Shear Strength of Concrete Deep Beams Reinforced with FRP Bars with/without Fibrous Concrete

Eklas Hatto Hashim *, ***Hassan Falah Hassan***
Civil Department, Engineering College, Mustansiriyah University, Baghdad, Iraq.

Keywords:
Deep beam; FRP reinforcement; Shear equations; Simply supported beam; Web reinforcement.

Highlights:
- *Deep beam analysis methods of the shear models put forth by the codes and searchers.*
- *The deep beam variables that effect on shear capacity.*
- *FRP reinforced deep beams.*

ARTICLE INFO
Article history:

Received	26 June 2023
Received in revised form	07 Oct. 2023
Accepted	13 Feb. 2024
Final Proofreading	30 July 2024
Available online	20 Mar. 2025

Citation: Hashim EH, Hassan HF. **Evaluating the Predicted Shear Strength of Concrete Deep Beams Reinforced with FRP Bars with/without Fibrous Concrete**. *Tikrit Journal of Engineering Sciences* 2025; **32**(1): 1112.
http://doi.org/10.25130/tjes.32.1.12

***Corresponding author:**

Eklas Hatto Hashim
Civil Department, Engineering College, Mustansiriyah University, Baghdad, Iraq.

Abstract: One of the typical and significant components of large structural superstructures, such as offshore structures, bridges, and large multistory buildings, is the reinforced concrete deep beam. A deep beam is mostly used to transfer load foundations, girders, bending and pile caps, and some walls. Numerous studies have been done on the deep beams' behavior under stresses because of the significance of deep beams. Even there are specifications for fiber-reinforced Polymers (FRP) reinforced deep beam in some codes, along with suggestions for the method prediction of load failure, strut-tie method (STM) method, included in most codes. It should be noted that many studies are still re-evaluating the factors utilized in the analysis method. The paper offers deep beam analysis methods of the shear models proposed by the codes and searcher for some published research. The survey database of 120 FRP-reinforced deep beams tested in shear was used to conduct the study. All specimens simply supported beams under three or four points load and rectangular cross-section. The specimens studied included different web shear reinforcement (horizontal and vertical), compressive strength, shear span-to-depth ratio a/d, and fiber volume fraction. Models combining steel and FRP reinforcement were excluded. The models predicting the shear capacity of FRP reinforced deep beams evaluated in this study were STM of CSA S806-12, Shear capacity V_c of ACI 440-11-22 and CSA S806-12, Zhang et al. [31] model, and Nehdi et al. [32] model. The models predicting the shear capacity of FRP reinforced deep beam evaluated in this study were either unsafe or inaccurate. The shear strength prediction of STM CSA S806 was most appropriate; however, it is conservative, making it uneconomical. Zhang et al. [31] presented a shear strength prediction model for FRP-reinforced deep beams without web reinforcement. No method is recommended for calculating the effect of fiber volume fraction on the shear capacity of FRP-reinforced concrete deep beams.

تقييم قوة القص المتوقعة للعتبات الخرسانية العميقة المسلحة بقضبان او بدون خرسانة ليفية مع قضبان الالياف البوليمرية

اخلاص هاتو هاشم، حسن فلاح حسن
قسم الهندسة المدنية/ كلية هندسة / الجامعة المستنصرية / بغداد - العراق.

الخلاصة
العتبات الخرسانية العميقة هي أحد المكونات النموذجية والهامة للهياكل الفائقة الكبيرة، مثل الهياكل البحرية والجسور والمباني الكبيرة متعددة الطوابق. يتم استخدام العتبات العميقة في الغالب لنقل احمال الأساسات والجسور وأغطية الركائز وبعض الجدران. تم إجراء العديد من الأبحاث والدراسات حول سلوك العتبات العميقة تحت الاجهادات المختلفة وذلك لأهميتها. تجدر الإشارة إلى أن العديد من الأبحاث لا تزال تعيد تقييم العوامل المستخدمة في طريقة التحليل رغم أن هناك مواصفات العتبات العميقة المسلحة بقضبان الألياف البوليمرية (FRP) في بعض المدونات، إلى جانب اقتراحات لطريقة التنبؤ بحمل الفشل، وطريقة رباطات الشد ودعامات الانضغاط (STM) والتي تم تضمينها في معظم المدونات. يقدم هذا البحث طرق تحليل الشعاع العميق لنماذج القص التي تقدمها بعض المدونات والباحثين في عدد من بعض الأبحاث المنشورة. تم استخدام قاعدة البيانات لـ ١٢٠ عتبة عميقة ذات اسناد بسيط ومسلحة بقضبان FRP تم اختبارها في القص لإجراء هذه الدراسة. جميع العينات لعتبات مسندة ببساطة تحت حمل ثلاث أو أربع نقاط وذات مقطع عرضي مستطيل. تضمنت العينات المستخدمة متغيرات تقوية القص (الأفقي والرأسي)، مقاومة الضغط، نسبة امتداد القص إلى العمق a/d ونسبة حجم الألياف. تم استبعاد النماذج التي تجمع بين تسليح الفولاذ وFRP. نماذج التنبؤ بقدرة القص للعتبات العميقة المسلحة بقضبان FRP والتي تم تقييمها في هذه الدراسة هي STM لـ CSA S806-12، وسعة القص V_c لـ ACI 440-11-22 و CSA S806-12، ونموذج .Zhang et al ونموذج .Nehdi et al. إن نماذج التنبؤ بقدرة القص للعتبات العميقة المسلحة بـ FRP والتي تم تقييمها في هذه الدراسة هي إما غير آمنة أو غير دقيقة. يعد التنبؤ بقوة القص لـ STM CSA S806 هو الأكثر ملاءمة ولكنه متحفظ مما يجعله غير اقتصادي بعض الشيء، في حين أن نموذج .Zhang et al يقدم نموذج التنبؤ بقوة القص للعتبات العميقة المسلحة بـ FRP غيرالمسلحة لمقاومة القص. لا توجد طريقة موصى بها لحساب تأثير جزء حجم الألياف على قدرة القص للعتبات الخرسانية العميقة المسلحة ب FRP.

الكلمات الدالة: العتبات العميقة، التسليح باستخدام قضبان FRP، معادلات القص، العتبات الاسناد البسيط، تسليح القص.

1.INTRODUCTION

Deep beams are defined as members with a smaller span than their depth. ACI 318-19 code considers the beam to have either a clear span $l_n \leq 4.0$ height of beam section h or a shear span $a \leq 2.0h$ as a deep beam. CSA A23.3-19 code considers the beam deep when $l_n \leq 2.0h$. The common loading types in deep beams are mostly concentrated point loads due to their unique structural characteristics and use cases. Critical shear zones are often created nearby due to the load's concentration at one or two places. Deep beams must be designed for these shear conditions if structural safety is to be assured. The strain distribution over the cross-section of a deep beam cannot be regarded as linear; there will be noticeable shear deformation compared to pure flexure. Typically, shear, rather than flexure, governs deep beam strength. The concrete contribution to the shear capacity is assumed through resistance across the concrete compressive zone, dowel action, and aggregate interlock [1]. The shear transmission processes, consequently, failure modes differ in deep beams compared to slender beams. While deep beams have a significant reserve of strength following developing diagonal cracks due to developing the arching mechanism, slender beams without stirrups fail soon after diagonal cracks appear. Additionally, deep beams are almost designed based on member analysis employing strut and tie modeling, whereas the slender beams shear design in design codes is based on sectional analysis [2, 3]. Since the deep beam structure's behavior consists of discontinuity or disturbed regions (D-region, as shown in Detail 1), the strut and ties (STM) model is a good method for predicting strength [4-6].

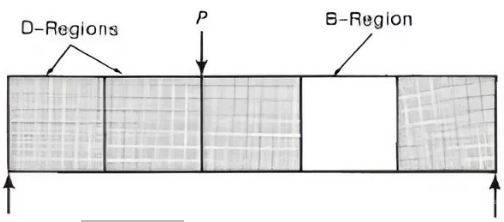

Detail 1 D - Region of Beam.

The model components' strengths parameter is expressed by the strength of ties, struts, and nodes. However, it is difficult to define an appropriate strut-and-tie model when shear reinforcement is present, or many point loads are applied close to the supports, and existing shear strength calculation models of RC deep beam exhibit high conservatism. Also, the choice of the strut and ties model is made at the designer's discretion, i.e., it may not be a unique solution. For these reasons, many studies have been conducted on predicting the shear capacity of deep beams, improving the STM method, calculating shear strength for deep beams, or evaluating the code provisions predicting the shear strength of FRP-reinforced deep beams [7, 8]. A reinforced deep beam's shear strength depends on several factors. The present study discussed the factors representing the parameters necessary for accurately predicting the shear capacity of deep beams. The parameters discussed are concrete compressive strength f_c', height of beam section h, a/d, longitudinal reinforcement ratio ρ, with or without web reinforcement ρ_w, and the modulus of elasticity of FRP bar E_f. To evaluate some existing shear strength calculation models of RC deep beam, experimental shear strength/ calculated the shear strength *(Vexp / Vcalc)* ratio used. Predicting the shear strength model is conservative if the ratio *Vexp/ Vcalc* is greater than 1, and it is unsafe if *Vexp / Vcalc* is less than 1.

2.RESEARCH SIGNIFICANCE

The present study describes the variables influencing the shear strength of FRP-reinforced concrete deep beams. Also, the study evaluates a calculation method for the shear strength of FRP-reinforced deep beams using available codes and researchers' equations. The evaluation is important to determine which method is best for calculating the shear strength of FRP-reinforced deep beams. The study reviewed available research data for FRP-reinforced concrete deep beams, the variation in the deep beams specimens' properties, and the effect of these properties on predicting shear capacity. The provisions' predicted values were compared with the experimental shear capacity in the literature.

3.EXPERIMENTAL DATA

The steel corrosion problem is one of the important considerations of the FRP bar reinforcement used instead of steel. The tensile strength of the FRP is greater than steel. Depending on the type of fibers used, the level of manufacture, and the particular application, the specific tensile strength of an FRP material can vary significantly. Also, using FRP reinforcement improves the chemical and chloride ion attack in addition to other considerations mentioned in more detail in ACI 440.1R-15 [9]. Standards for designing and constructing building components with fiber-reinforced polymers were developed due to the material's expanding use in construction. No FRP RC deep beam specification can be found in ACI 440.1R-15 [9]. It submits a procedure to calculate the shear strength of the FRP RC deep beams in an example used in the present study. ACI 440.1R-15 [9] does not include STM for FRP reinforcement structure, also STM out of ACI 440.11-22 scope [10]. CSA S806 [11] presents STM and shear strength V_c for FRP reinforcement structure, which is close to CSA A23.3 [11,12]. Studies on FRP-RC deep beams with web reinforcement often use glass fiber-reinforced polymers (GFRP), the most available and cheapest [13-16]. Comparison research between different types of reinforcement found that the carbon fiber reinforced polymers (CFRP) RC deep beam has more shear strength than the GFRP-RC deep beam [17,18], and in comparison, to steel RC deep beam with FRP RC deep beam; the first is more ductile behavior [16, 19, 20]. The abbreviations of FRP types are listed in Table 1.

Table 1 Abbreviations of FRP Types.

Acronyms	Type
FRP	Fiber-reinforced polymer
AFRP	Aramid fiber-reinforced polymer
BFRP	Basalt fiber-reinforced polymer
CFRP	Carbon fiber-reinforced polymer
GFRP	Glass fiber-reinforced polymer

The experimental database includes 120 FRP RC deep beams tested for shear in some published studies used in the present study, including the four types of FRP: GFRP, CFRP, basalt fiber reinforced polymers (BFRP), and aramid fiber reinforced polymers (AFRP) are included in the study. All the specimens had a shear span to depth ratio *a/d* less than 2.5. Table 2 provides details of the FRP RC deep beam samples used in this study.

Table 2 FRP Reinforcement Specimen Properties.

No.	Researcher	Specimen	Type Rein.	b_w mm	h mm	a/d	f'_c MPa	ρ_w	f_u main MPa	ρ main	E_f main GPa	Fiber volume %	Vexp kN
1	El-Sayed et al. [17]	G-0.7/1.6	G	250	400	1.69	40.5	0	749	0.0078	42	0	164.5
2		G-1.2/1.6	G	250	400	1.69	40.5	0	749	0.0124	42	0	175
3		G-1.7/1.6	G	250	400	1.69	40.5	0	749	0.0171	42	0	196
4		G-1.2/1.3	G	250	400	1.3	40.5	0	749	0.0124	42	0	269
5		G-1.2/0.9	G	250	400	0.92	40.5	0	749	0.0124	42	0	450.5
6	Abed et al. [19]	B1-FRP	G	200	300	1.08	43	0	1050	0.0092	51	0	153.4
7		B2-FRP	G	200	300	1.3	43	0	1050	0.0092	51	0	130.8
8		B3-FRP	G	200	300	1.52	43	0	1050	0.0092	51	0	116.55
9		B4-FRP	G	200	300	1.08	43	0	1050	0.0138	51	0	182.8
10		B5-FRP	G	200	300	1.08	43	0	1050	0.0184	51	0	230.35
11		B6-FRP	G	200	350	1.04	43	0	1050	0.0112	51	0	157.4
12		B7-FRP	G	200	400	1	43	0	1050	0.0126	51	0	216.3
13		B8-FRP	G	200	300	1.08	51	0	1050	0.0092	51	0	220.8
14		B9-FRP	G	200	300	1.08	65	0	1050	0.0092	51	0	237.35
15	Farghaly and Benmokrane [18]	G8N6	G	300	1200	1.13	49.3	0	790	0.0069	47.6	0	723.5
16		G8N8	G	300	1200	1.13	49.3	0	750	0.0124	51.9	0	953
17	Andermatt and Lubell [21]	A1N	G	310	306	1.07	40.2	0	709	0.0149	41.1	0	407
18		A2N	G	310	310	1.44	45.4	0	709	0.0147	41.1	0	235.5
19		A3N	G	310	310	2.02	41.3	0	709	0.0147	41.1	0	121.5
20		A4H	G	310	310	2.02	64.6	0	709	0.0147	41.1	0	96
21		B1N	G	300	608	1.08	40.5	0	765	0.017	37.9	0	636.5
22		B2N	G	300	606	1.48	39.9	0	765	0.017	37.9	0	399.5
23		B3N	G	300	607	2.07	41.2	0	765	0.017	37.9	0	215.5
24		B4N	G	300	606	1.48	40.7	0	709	0.0213	41.1	0	415
25		B5H	G	300	607	1.48	66.4	0	709	0.0212	41.1	0	531
26		B6H	G	300	610	2.06	68.5	0	765	0.017	37.9	0	188
27		C1N	G	301	1003	1.1	51.6	0	938	0.0158	42.3	0	1134.5
28		C2N	G	304	1005	1.49	50.7	0	938	0.0156	42.3	0	662

29		A1/100	G	230	675	1	49.8	0.0028	656	0.01197	47.6	0	560.25
30		A1/75	G	230	675	1	52.2	0.0019	656	0.01197	47.6	0	552.39
31		A1/50	G	230	675	1	52.5	0.00122	656	0.01197	47.6	0	493.69
32		A1/00	G	230	675	1	52.7	0	656	0.01197	47.6	0	416.89
33	Latosh [13]	B1.5/100	G	230	500	1.5	51.8	0.0029	708-656	0.01201	46.95	0	322.38
34		C2/100	G	230	375	2	50.8	0.00316	708	0.01	46.3	0	125.91
35		C2/75	G	230	375	2	51	0.0019	708	0.01	46.3	0	98.68
36		C2/50	G	230	375	2	51.3	0.0006	708	0.01	46.3	0	102.71
37		C2/00	G	230	375	2	51.3	0	708	0.01	46.3	0	93.47
38		B25	G	120	300	2	19.6	0	640	0.01131	46.25	0	54.91
39		B25-1	G	120	300	2	19.6	0.0039	640	0.01131	46.25	0	77.005
40		B25-2	G	120	300	2	19.6	0.0056	640	0.01131	46.25	0	65
41		B25-3	G	120	300	2	19.6	0.0084	640	0.01131	46.25	0	99.5
42	Said et al.	B45-1	G	120	300	2	38.4	0.0039	640	0.01509	46.25	0	115
43	[14]	B45-2	G	120	300	2	38.4	0.0056	640	0.01509	46.25	0	128.5
44		B45-3	G	120	300	2	38.4	0.0084	640	0.01509	46.25	0	152
45		B70-1	G	120	300	2	59.52	0.0039	640	0.02263	46.25	0	157.5
46		B70-2	G	120	300	2	59.52	0.0056	640	0.02263	46.25	0	130
47		B70-3	G	120	300	2	59.52	0.0084	640	0.02263	46.25	0	175.5
48		G1.13VH	G	300	1200	1.13	37	0.011	1000	0.0124	62.4	0	1,452
49		G1.47V	G	300	1200	1.47	45.4	0.0042	1000	0.0124	62.6	0	1,325
50		G1.13V	G	300	1200	1.13	44.6	0.0042	1000	0.0124	62.6	0	1,618
51		G0.83V	G	300	1200	0.83	43.6	0.0042	1000	0.0124	62.6	0	1,694
52	Mohamed et al. [15]	G1.47H	G	300	1200	1.47	45.4	0.0068	1000	0.0124	62.6	0	848
53		G1.13H	G	300	1200	1.13	44.6	0.0068	1000	0.0124	62.6	0	1,267
54		G0.83H	G	300	1200	0.83	43.6	0.0068	1000	0.0124	62.6	0	1,583
55		G1.13	G	300	1200	1.13	37	0	1000	0.0124	62.6	0	1,344
56		G1.47	G	300	1200	1.47	38.7	0	1000	0.0124	62.6	0	925
57		G0.83	G	300	1200	0.83	38.7	0	1000	0.0124	62.6	0	1,500
58		X-0.6	G	250	590	1.18	45	0	1184	0.006	62.6	0	358
59		X-1.0	G	250	590	1.18	47	0	1184-1105	0.01	63.15	0	400
60		X-1.4	G	250	590	1.18	46	0	1105	0.014	63.7	0	450
61	Bediwy et al. [22]	B-0.6	G	250	590	1.18	47	0	1184	0.006	62.6	Basalt 2.5	425.5
62		B-1.0	G	250	590	1.18	48	0	1184-1105	0.01	63.15	Basalt 2.5	450
63		S-0.6	G	250	590	1.18	46	0	1184	0.006	62.6	Steel 1	460
64		S-1.0	G	250	590	1.18	45	0	1184-1105	0.01	63.15	Steel 1	490.5
65		S1.5-G10-SF0-R10	G	150	150	1.5	54	0	1015	0.0089	49.8	Steel 0	57.5
66	Hosseini et al. [23]	S1.5-G10-SF0.75-R10	G	150	150	1.5	55	0	1015	0.0089	49.8	Steel 0.75	66.8
67		S1.5-G10-SF1.5-R10	G	150	150	1.5	54	0	1015	0.0089	49.8	Steel 1.5	71.5
68		GN6/0.5	G	170	500	0.5	28	0	680	0.017	42	0	415
69		GN6/0.75	G	170	500	0.75	30	0	650	0.017	39	0	265
70	Thomas and Ramadass	GN6/1.00	G	170	500	1	28.5	0	660	0.017	41	0	210
71	[24]	GN4/0.5	G	170	500	0.5	31.5	0	640	0.0114	40	0	350
72		GN4/0.75	G	170	500	0.75	32	0	645	0.0114	41.5	0	240
73		GN4/1.00	G	170	500	1	33	0	655	0.0114	39.5	0	190
74		SP3	G	150	500	1.33	40	0.00830	740	0.00232	46.25	0	212.75
75		SP4	G	150	500	1.33	40	0.00830	740	0.00348	46.25	0	268.75
76	Nassif et al.	SP5	G	150	500	1.33	40	0.00830	1075	0.00334	46.25	0	337.65
77	[16]	SP6	G	150	500	1.33	48	0.00830	740	0.00232	46.25	0	225.35
78		SP7	G	150	500	1.33	48	0.00830	740	0.00348	46.25	0	285.05
79		SP8	G	150	500	1.33	48	0.00830	1075	0.00334	46.25	0	360.2
80		C-0.7/1.6	C	250	400	1.69	39.4	0	986	0.0078	134	0	179.5
81	El-Sayed et al.	C-1.2/1.6	C	250	400	1.69	39.4	0	986	0.0124	134	0	195
82	[17]	C-1.7/1.6	C	250	400	1.69	39.4	0	986	0.0171	134	0	233.5
83		C-1.2/1.3	C	250	400	1.3	39.4	0	986	0.0124	134	0	372
84		C-1.2/0.9	C	250	400	0.92	39.4	0	986	0.0124	134	0	500
85	Farghaly and	C12N3	C	300	1200	1.13	38.7	0	1596	0.0026	120	0	595.5
86	Benmokrane [18]	C12N4	C	300	1200	1.13	38.7	0	1899	0.0046	144	0	800.5
87		C3D9M-1.4	C	200	290	1.4	26.1	0	1955.8	0.0038	120.2	0	84.63
88		C3D9M-1.7	C	200	290	1.7	26.1	0	1955.8	0.0038	120.2	0	53.27
89	Kim et al.	C3D9M-2.1	C	200	290	2.1	26.1	0	1955.8	0.0038	120.2	0	26.32
90	[20]	C4D9M-1.7	C	200	290	1.7	26.1	0	1955.8	0.0051	120.2	0	48.045
91		C5D9M-1.7	C	200	290	1.7	26.1	0	1955.8	0.0064	120.2	0	75.695
92		C3D9S-1.7	C	200	230	1.7	26.1	0	1955.8	0.005	120.2	0	52.42
93		C5D9L-1.7	C	200	350	1.7	26.1	0	1955.8	0.0051	120.2	0	72.695
94		BF-1	B	200	300	1.54	41	0	1123	0.0077	51.3	0	120.1
95		BF-2	B	200	300	1.73	41	0	1123	0.0077	51.3	0	90.9
96		BF-3	B	200	300	2.02	41	0	1123	0.0077	51.3	0	83.8
97	Liu et al.	BF-4	B	200	300	1.54	41	0	1123	0.0092	51.3	0	144.4
98	[25]	BF-5	B	200	300	1.54	41	0	1123	0.0116	51.3	0	134
99		BF-6	B	200	350	1.29	41	0	1123	0.0076	51.3	0	178.2
100		BF-7	B	200	400	1.11	41	0	1123	0.0084	51.3	0	237.2
101		BF-8	B	200	300	1.54	52	0	1123	0.0077	51.3	0	128.5
102		BF-9	B	200	300	1.54	64	0	1123	0.0077	51.3	0	133.9
103		B1-BFRP	B	140	260	1.15	40	0	1230	0.0075	46.2	0	106.5
104	Alhamad et al. [26]	B2-BFRP	B	140	260	1.48	40	0	1230	0.0075	46.2	0	29.6
105		B3-BFRP	B	140	260	1.82	40	0	1230	0.0075	46.2	0	39.75

106		BN10-1.15	B	150	260	1.15	45	0	1227	0.0049	46.1	Basalt 0.8	165.41
107		BN12-1.15	B	150	260	1.15	45	0	1230	0.007	46.3	Basalt 0.8	192.89
108		BN16-1.15	B	150	260	1.15	45	0	1177.3	0.0126	46	Basalt 0.8	150.22
109	Abed et al. [27]	BN12-1.48	B	150	260	1.48	45	0	1230	0.007	46.3	Basalt 0.8	165.07
110		BN12-1.82	B	150	260	1.82	45	0	1230	0.007	46.3	Basalt 0.8	94.695
111		BH10-1.15	B	150	260	1.15	60	0	1227	0.0049	46.1	Basalt 0.8	207.44
112		PN10-1.15	B	150	260	1.15	45	0	1227	0.0049	46.1	0	95.755
113		SN10-1.15	B	150	260	1.15	45	0	1227	0.007	46.1	Synth.0.8	154.89
114		A3D9M-1.4	A	200	290	1.4	26.1	0	1826.9	0.0038	80.7	0	68.025
115		A3D9M-1.7	A	200	290	1.7	26.1	0	1826.9	0.0038	80.7	0	49.49
116	Kim et al. [20]	A3D9M-2.1	A	200	290	2.1	26.1	0	1826.9	0.0038	80.7	0	44
117		A4D9M-1.7	A	200	290	1.7	26.1	0	1826.9	0.0051	80.7	0	60.5
118		A5D9M-1.7	A	200	290	1.7	26.1	0	1826.9	0.0064	80.7	0	133.97
119		A3D9S-1.7	A	200	230	1.7	26.1	0	1826.9	0.005	80.7	0	54.79
120		A5D9L-1.7	A	200	350	1.7	26.1	0	1826.9	0.0051	80.7	0	67.135

4.DATABASE SUMMARY

The database specifications for the FRP reinforcement deep beam specimen used in this study differ significantly. Figure 1 represents the parameters of concrete compressive strength f_c', height of beam section h, a/d, longitudinal reinforcement ratio ρ, with or without web reinforcement ρ_w, and type of FRP. Table 3 summarizes the FRP RC deep beam database properties and the coefficient of variation COV.

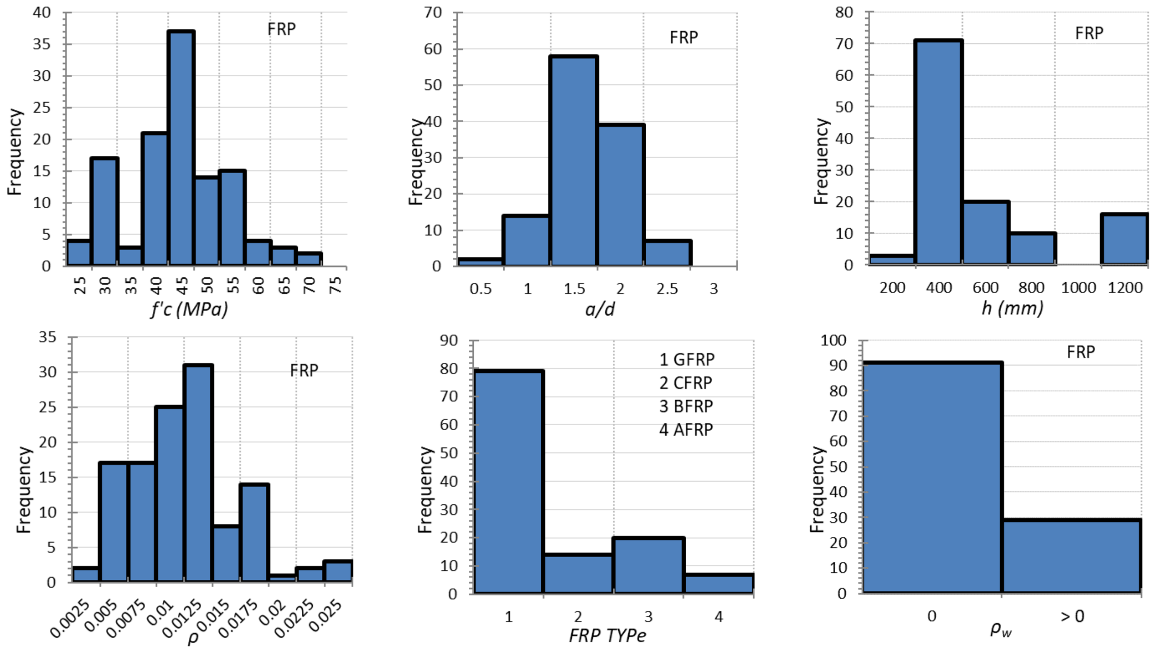

Fig. 1 Variable Distribution of Data Base of FRP RC Deep Beam.

Table 3 The Summary of FRP RC Deep Beam Data Base Properties.

	Without Web Reinforcement Data 91 Beam				With Web Reinforcement Data 29 Beam			
Properties	Min	Max	Mean	COV%	Min	Max	Mean	COV%
h (mm)	150	1200	448.77	59.49	300	1200	612.07	58.29
a/d	0.5	2.1	1.39	26.17	0.83	2	1.53	28.11
b_w (mm)	120	310	220. 50	24.17	120	300	196.21	37.11
f_c' (MPa.)	19.6	68.5	41.26	24.80	19.6	59.52	44.14	23.97
f_u (MPa)	640	1955.8	1127.35	34.99	640	1075	781.72	21.11
E_f (GPa)	37.9	144	62.88	47.09	46.25	62.6	50.36	13.95
ρ	0.0026	0.0213	0.0101	43.98	0.0023	0.0226	0.0114	48.49
ρf_u (MPa)	4.15	19.32	10.05	27.68	1.72	14.48	8.62	45.97
ρ_w	-	-	-	-	0.0006	0.011	0.0056	48.75
$\rho_w f_u$(MPa)	-	-	-	-	0.53	12.00	4.39	56.36

where b_w is the width of the beam section, f_u is the ultimate tensile strength of the FRP bar, and E_f is the modulus of elasticity of the FRP bar.

5.SELECTION MODELS OF SHEAR STRENGTH CALCULATION

Many studies still cover predicting the shear strength of FRP-reinforced deep beams. However, a few have studied this type of beam; however, they are still very conservative or inadequate in predicting its shear strength.

The present study of the concrete shear strength calculation for FRP reinforcement deep beam selected the recommendations using STM of CSA S806-12, Shear capacity V_c of ACI 440-11-22 [10] and CSA S806-12 [11], Zhang et al. [31] model, and Nehdi et al. [32] model, as the following:

5.1.Shear Concrete Capacity V_c of ACI 440.11- 22

According to ACI 440.1R-15 [9], the shear strength prediction method for slender beams for FRP is similar to steel-RC beams, considering the difference between the modulus of elasticity for steel and FRP. For shear capacity, the size effect component is included in ACI 440.11-22 [10] as follows:

$$V_c = 0.42\sqrt{f'_c} b_w \lambda_s k d \quad (1)$$

$$k = \sqrt{2\rho_f n_f + (\rho_f n_f)^2} - \rho_f n_f \quad (2)$$

$$n_f = \frac{E_f}{E_c} \quad (3)$$

$$\lambda_s = \sqrt{\frac{2}{1+0.004d}} \leq 1.0 \quad (4)$$

where ρ_f is the longitudinal reinforcement ratio, E_c is the modulus of elasticity of concrete, and λ_s is the size effect modification factor

5.2.Concrete Strength Capacity V_c Prediction and STM Method of CSA S806-12

5.2.1.Shear Concrete Capacity V_c of CSA S806-12

The Canadian code CSA S806-12 [11] considers the arch action effect on member shear strength by coefficients that consider the effect of the arch action k_a and the size effect by coefficient factor k_s, the effect of moment at section k_m, and the effect of reinforcement rigidity on its shear strength k_r.

$$V_c = 0.05\lambda k_m k_r k_a k_s (f'_c)^{1/3} b_w d_v \quad (5)$$

$$k_m = \sqrt{d/a} \leq 1.0 \quad (6)$$

$$k_r = 1 + (E_f \rho_f)^{1/3} \quad (7)$$

$$1.0 \leq k_a = 2.5/(d/a) \leq 2.5 \quad (8)$$

$$k_s = 750/(450 + d) \leq 1.0 \quad (9)$$

$$0.11\sqrt{f'_c} b_w d_v \leq V_c \leq 0.22\sqrt{f'_c} b_w d_v \quad (10)$$

where λ is the concrete density account factor, d is the effective depth, and d_v is the effective shear depth.

5.2.2.Strut and Tie Beam Method STM of CSA S806-12

The Canadian code CSA S806-12 [11] recommends STM for FRP-reinforced members as CSA A23.3-19 [12] for steel-reinforced members. The structure is idealized as a series of concrete compressive strength and reinforcing FRP tensile ties to form a truss interconnected at nodes. The truss must support the loads [28, 29]. This approach implies that the structure design is done according to the theory of plasticity's lower bound theorem [30]. The effect of web reinforcement is not accounted for in STM for simply supported deep beams.

Struts compressive strength F_{ns}:

$$F_{ns} = \phi_c f_{cu} A_{cs} \quad (11)$$

$$f_{cu} = \frac{f'_c}{0.8+170\varepsilon_1} \quad (12)$$

$$\varepsilon_1 = \varepsilon_f + (\varepsilon_f + 0.002)cot^2\theta_s \quad (13)$$

Tie tensile strength F_{nt}:

$$F_{nt} = 0.65\phi_F f_{Fu} A_{FT} \quad (14)$$

Compressive nodal zone F_{nn}:

$$F_{nn} = \phi_c \beta_n f'_c A_{nz} \quad (15)$$

$$\beta_n = \begin{cases} 0.85 \text{ for nodal zone bounded by bearing area and strut} \\ 0.75 \text{ for nodal zone anchoring one tie} \\ 0.65 \text{ for nodal regions anchoring more than one ties} \end{cases} \quad (16)$$

where ϕ_c is the resistance factor for concrete, A_{cs} is the concrete strut cross-section area, ε_f is the tensile strain in the tie bar, θ_s is the smallest angle that can be made between a strut and its adjacent ties, ϕ_F is the FRP reinforcement' resistance factor, f_{Fu} is the ultimate strength of FRP reinforcement, A_{FT} is the longitudinal FRP reinforcement area in the tension tie, and A_{nz} is the nodal zone face area.

5.3.Shear Concrete Capacity V_c

Zhang et al. [31] derived a generic closed-form solution from a segmental approach mechanics for shear capacity quantification of RC beams without stirrups for any type of reinforcement and concrete.

$$V_c = \frac{0.345 b_w n\rho d\left(\sqrt{1+\frac{2}{n\rho}}-1\right) f'^{\,0.665}_c}{1-\frac{Dd}{d-0.333n\rho d\left(\sqrt{1+\frac{2}{n\rho}}-1\right)}} \text{ for } \frac{a}{d} < 3.14 \quad (17)$$

$$n = \frac{E_f}{E_c} \quad (18)$$

$$D = -0.195\left(\frac{a}{d}\right)^2 + 0.511\left(\frac{a}{d}\right) + 0.212 \quad (19)$$

5.4.Shear Capacity V_n

Nehdi et al. [32] proposed a simple improved formula based on a genetic algorithms technique to determine the shear capacity of a concrete deep beam reinforced with FRP. The authors also showed that a cubic root function, rather than a linear function, was the best fit to describe the FRP longitudinal bars' axil rigidity, and the FRP stirrups' contribution to shear strength was a square root function of the ultimate capacity of stirrups.

$$V_n = V_{cf} + V_{fv} \quad (20)$$

$$V_{cf} = 2.1\left(\frac{f'_c \rho_{fl} d}{a}\frac{E_{fl}}{E_s}\right)^{0.3} b_w d \times 2.5\frac{d}{a} \text{ for } \frac{a}{d} < 2.5 \quad (21)$$

$$V_{fv} = 0.5(\rho_{fv} f_{fv})^{0.5} \quad (22)$$

where V_{cf} is the shear capacity of concrete beam reinforced with FRP without web reinforcement, V_{fv} is the FRP stirrups' shear capacity, ρ_{fl} is the longitudinal reinforcement ratio, E_{fl} is the modulus of elasticity of FRP bar, E_s is the modulus of elasticity of steel, ρ_{fv} is the shear reinforcement ratio, f_{fv} is the ultimate capacity of shear reinforcement. Nehdi et al. [32] calculated only the vertical web reinforcement contribution. Because the web reinforcement for the specimens in this study was not always vertical, the shear capacity of the horizontal web reinforcement model given by Nehdi et al. [32] was not included in the evaluation.

6.SUMMARY OF THE PERFORMANCE METHODS

A summary of the performance methods adopted in the present study for experimental data of FRP reinforced concrete deep beam is shown in Table 4. The coefficient of variation COV of *Vexp / Vcalc* of the STM method of CSA S806-12 [11] is good (between 20-30) compared with the other methods, making it better than the other methods. The COV value of *Vexp/ Vcalc* for the other methods was greater than 30, meaning that the result was dispersion for the same method for different FRP-reinforced concrete deep beam properties.

Table 4 *Vexp/Vcalc* of Methods Adopted in the Present Study for Experimental Data of FRP RC Deep Beam.

Method	Without Web Reinforcement Data 91 Beam *Vexp/Vcalc*				With Web Reinforcement Data 29 Beam *Vexp/Vcalc*			
	Min	Max	Mean	COV%	Min	Max	Mean	COV%
ACI 440.11-22 V_c [10]	1.386	13.203	6.121	44.504	-	-	-	-
CSA S806-12 STM [11]	0.968	6.387	3.178	28.882	1.984	10.558	5.379	40.320
CSA S806-12 V_c [11]	0.552	2.860	1.408	32.962	-	-	-	-
Zhang et al. V_c [31]	0.537	4.765	1.868	48.849	-	-	-	-
Nehdi et al. [32]	0.613	3.479	1.508	35.076	-	-	-	-

7.SHEAR STRENGTH MODELS PERFORMANCE VERSUS AFFECTING FACTORS

The STM for FRP is out of ACI 440.11-22 [10] scope. The shear strength of the specimen with web reinforcement was only calculated using STM of CSA S806-12 [11]. The shear strength was calculated for specimens without web reinforcement by using STM of CSA S806-12 [11], Shear capacity V_c of ACI 440.11-22 [10] (for slender beam) and CSA S806-12 [11], Zhang et al. [31] model, and Nehdi et al. [32] model. The model is written at the top right of all drawings of the relation between *Vexp/Vcalc* and effecting factors, where (+w) means with web reinforcement, and (ow) means no web reinforcement.

7.1.Concrete Compressive Strength f'_c

The compressive strength of concrete f'_c is the main parameter in calculating shear concrete capacity V_c. When the stress exceeds the allowable stress of concrete and an inclined crack forms, shear failure occurs. The presence of web reinforcement delays or limits the development of the cracks. The average of the shear strength predictions varied for all concrete compressive strength values f'_c, as shown in Fig. 2 a, b, c, d, e, and f for specimens with and without web reinforcement, respectively.

7.2.Shear Span to Depth Ratio a/d

Considering whether the beam is slender or deep is limited by the ratio of shear span to depth a/d. The shear strength decreased as the a/d ratio increased, which is an important factor in this regard [6, 33]. Figure 3 shows the relation between *Vexp/Vcalc* and the a/d ratio for the beam. The shear strength by the STM method of CSA S806-12 [11] was more conservative than the other method.

7.3.Height of Cross Section Beam h

Increasing beam height decreased the shear strength for the FRP RC deep beam. The beam with large h/b showed a higher flexural crack propagation rate. The proper strut geometry design decreased the size effect by appropriate plate support and loading dimensions [34]. Figure 4 shows the change in *Vexp / Vcalc* with beam height increase for the specimen.

7.4.Longitudinal Reinforcement Ratio ρ

The shear strength increased when the longitudinal reinforcement ratio increased. With a low reinforcement ratio, wider and deeper cracks occurred. Deeper cracks decreased the depth of the uncracked compression zone of concrete, thus decreasing the uncracked concrete's contribution to the shear. The FRP reinforcement showed no dowel action. An accurate description of the FRP longitudinal reinforcement ρ ratio effect is the equivalent force of longitudinal reinforcement, as known because the ultimate tensile force varied with the diameter, i.e., ρf_u. The relations between the *Vexp / Vcalc* ratio and the longitudinal reinforcement ρ ratio are shown in Fig. 5. The relations between the *Vexp / Vcalc* ratio and the longitudinal reinforcement ρf_u ratio are shown in Fig. 6. The shear strength predictions for all models are conservative for ρ and ρf_u.

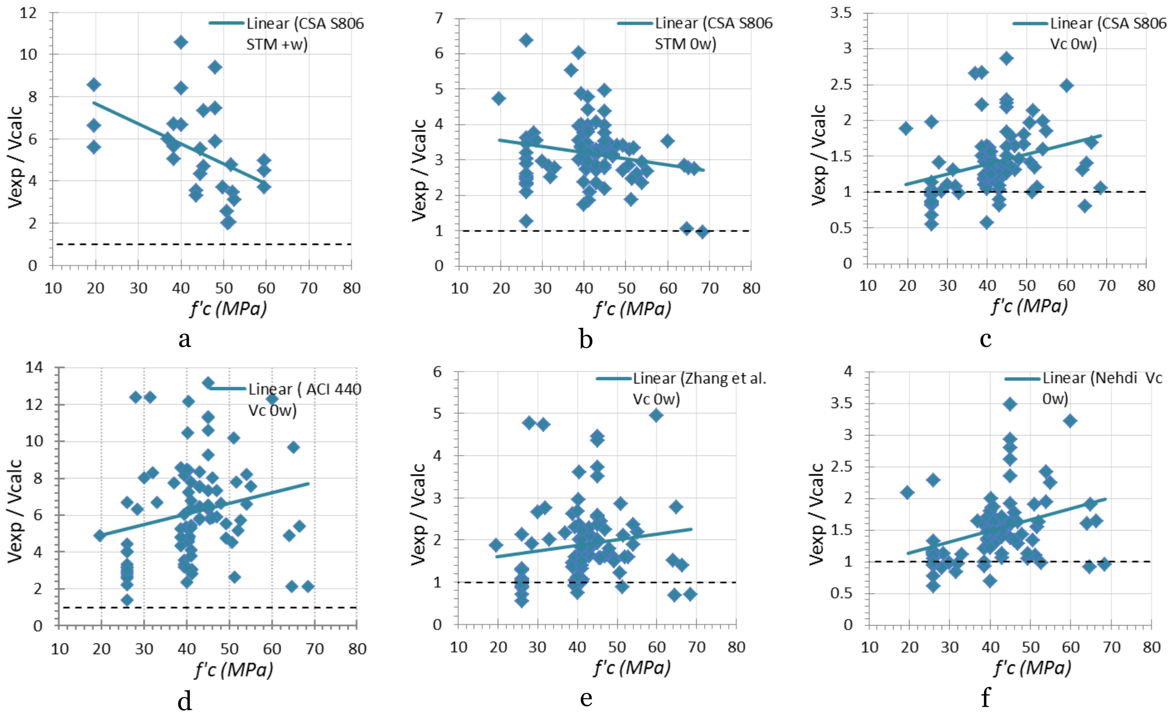

Fig. 2 The Relation between *Vexp/Vcalc* and Compressive Strength f_c' for FRP RC Deep Beam.

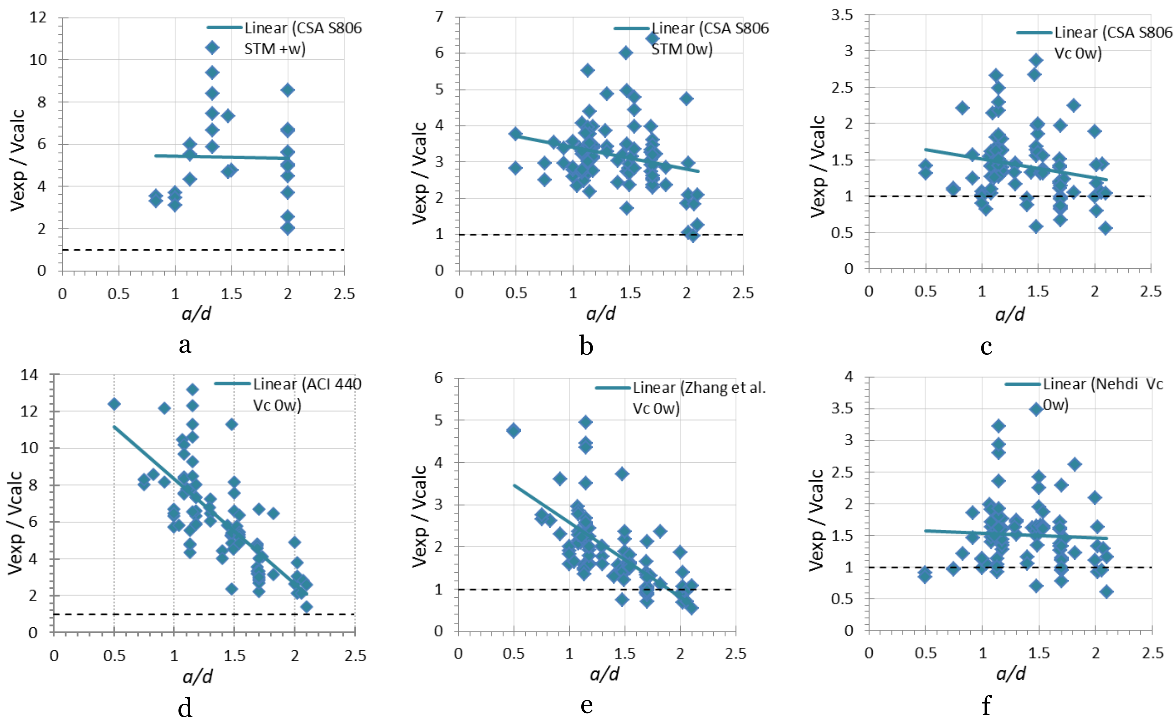

Fig. 3 The Relation between *Vexp / Vcalc* and *a/d* for FRP RC Deep Beam.

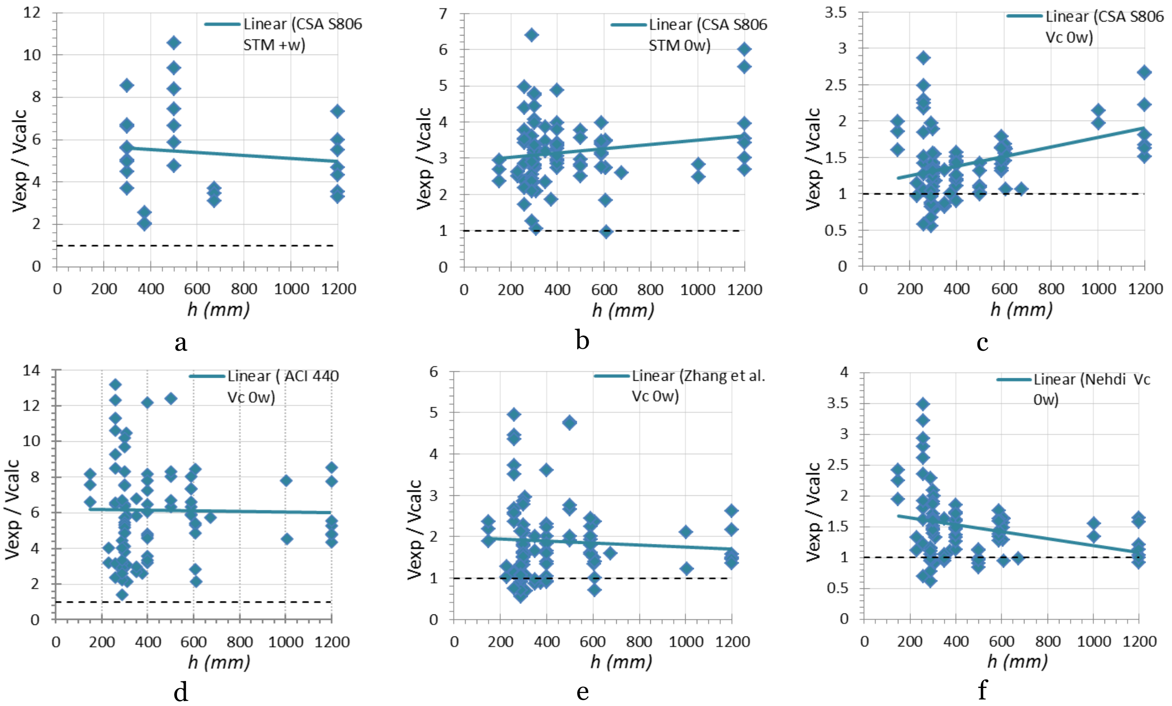

Fig. 4 The Relation between *Vexp / Vcalc* and Height *h* of Cross Section of FRP RC Deep Beam.

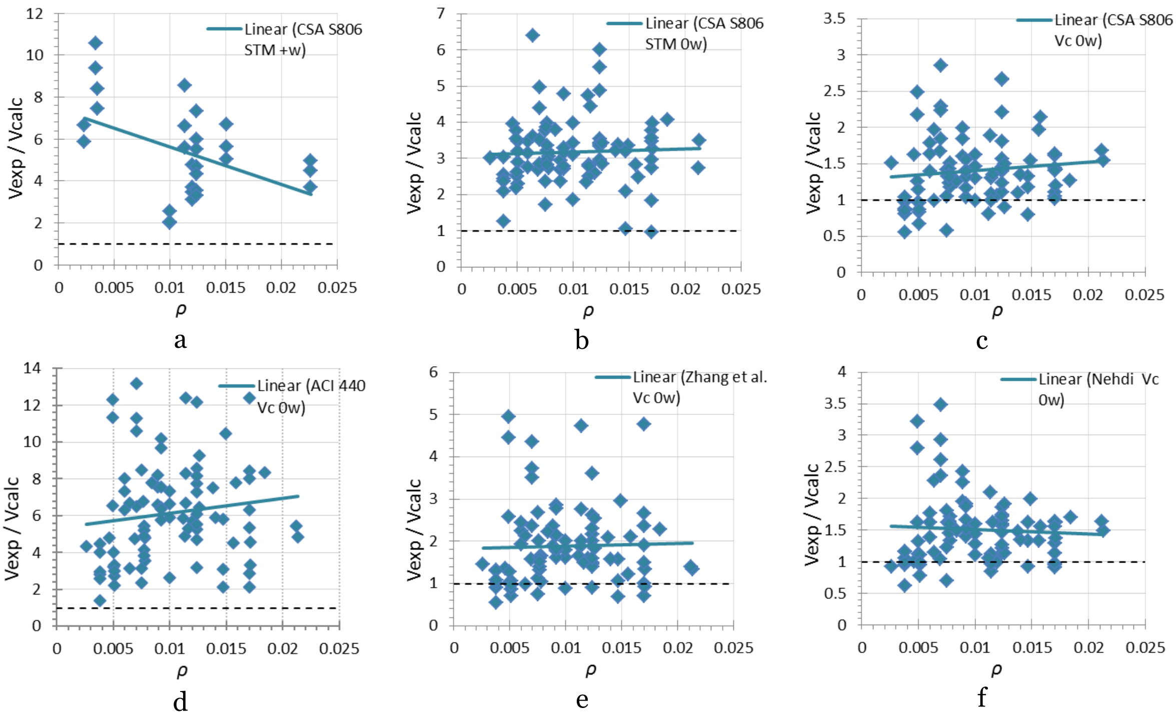

Fig. 5 The Relation between *Vexp / Vcalc* and Longitudinal Reinforcement ρ of FRP RC Deep Beam.

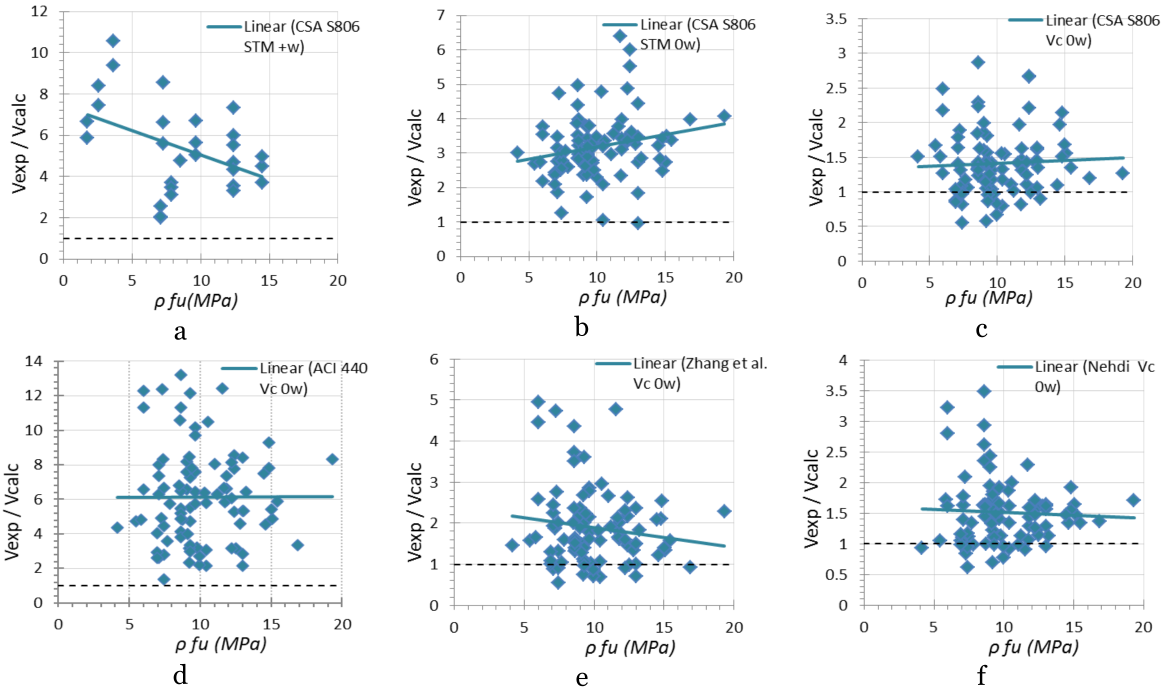

Fig. 6 The Relation between *Vexp / Vcalc* and the Ultimate Force of Longitudinal Reinforcement ρf_u of an FRP RC Deep Beam.

7.5.Web Reinforcement Ratio ρ_w

Generally, most of the shear prediction methods assume that the contribution of FRP shear reinforcement is the same way as steel shear reinforcement contribution, i.e., the shear or web reinforcement carries the shear after developing diagonal cracks. The CSA S806-12 [11] recommends using minimum reinforcement requirements to control the crack; however, that recommendation is inaccurate, as the diameter of the FRP bar was not specified, and it is known that the ultimate tensile force varies according to the diameter. Figure 7 shows the *Vexp/Vcalc* ratio relation with web reinforcement ρ_w and $\rho_w f_u$ for the STM CSA S806-12 [11] model. Samples included GFRP RC deep beam only as it is the only type available with web reinforcement.

7.6.FRP Modulus of Elasticity E_f

Although the FRP bars' tensile strength was greater than that of steel bars, their modulus of elasticity was lower. The type of fiber controls the modulus of elasticity of FRP bars. The *Vexp/Vcalc* ratio relation with modulus of elasticity E_f is shown in Fig. 8.

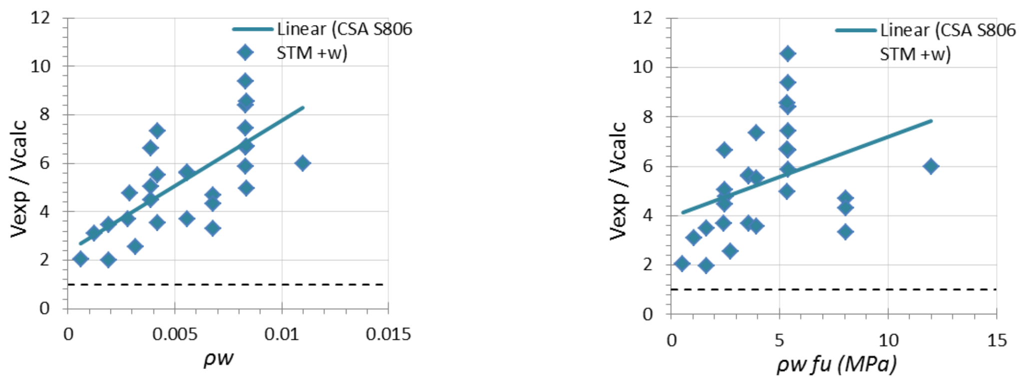

Fig. 7 The Relation between *Vexp/ Vcalc* and Web Reinforcement ρ_w and $\rho_w f_u$ of FRP RC Deep Beam.

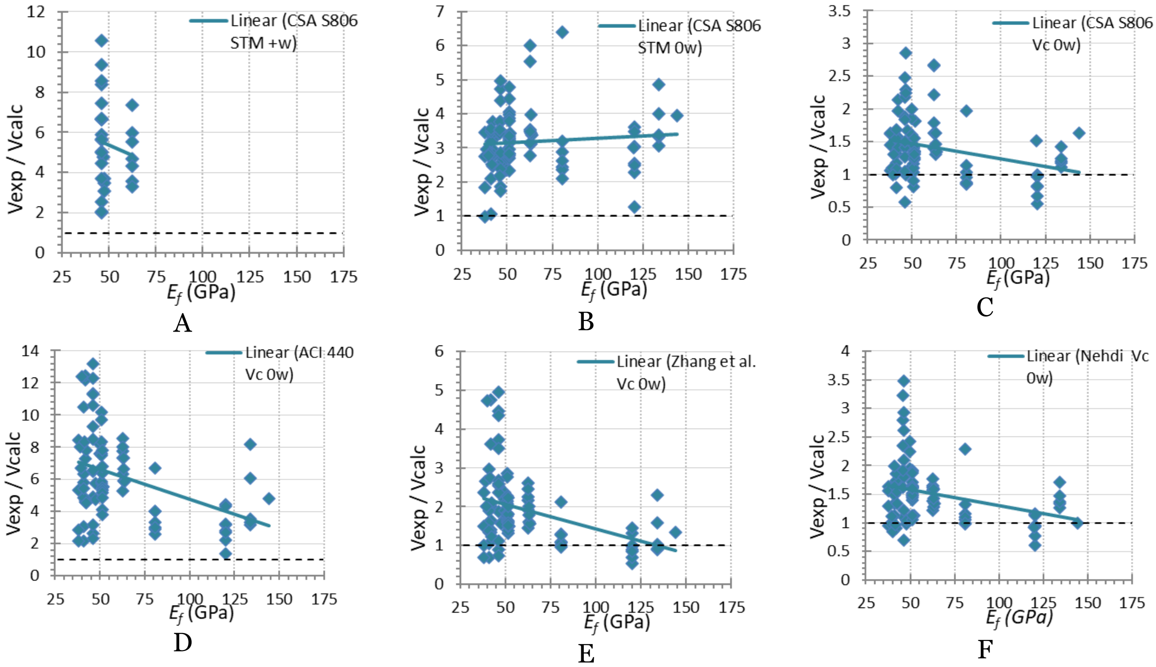

Fig. 8 The Relation between *Vexp / Vcalc* and Modulus of Elasticity E_f of FRP RC Deep Beam.

7.7.Fiber Effect

Studies investigating the fiber influence in FRP RC deep beams are limited. The fibrous FRP RC beam of the database is shown in Fig. 9. The indirect effect of fiber in deep beams is the effect on concrete properties like compressive strength f_c' and concrete tensile strength f_t. Since the fiber affects the behavior of reinforced concrete beams in general and FRP RC deep beams especially, more studies are required to consider this effect.

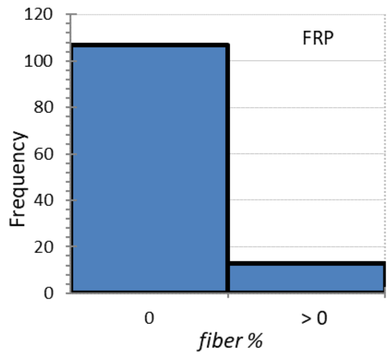

Fig. 9 The Fibrous FRP RC Beam of the Data Base.

8.CONCLUSIONS

In most cases, the steel-RC shear design provisions are modified to include details relevant to the FRP material and FRP-RC behavior. Due to the difference between the properties of FRP bars and steel bars, using the same analysis, design mechanism, and philosophy of steel used for FRP is inappropriate. In this study, a database of 120 FRP RC deep beam specimens from 18 studies was used to evaluate the performance of the models of V_c ACI 440-11-22 [10], STM and V_c of CSA S806-12 [11], Zhang et al. [31], and Nehdi et al. [32]. The accuracy of predicting methods of the shear strength of FRP RC deep beams, discussed in the current study, is affected by the parameters f_c', h, a/d, ρ, ρ_w, and E_f. In the STM CSA S806-12 [11] model, the shear strength predicting (for beams with web reinforcement) is affected by the change of f_c', h, ρ, ρ_w, and E_f, and the predicting is constant with a change of a/d. In contrast, the predicting of STM CSA S806-12 [11] (for beams without web reinforcement) model is affected by the shift in f_c', h, and ρ_w, and the predicting is constant with the change of ρ and E_f. CSA S806-12 [11] shear strength predicting models (V_c for beams without web reinforcement) are affected by changes in all parameters, meaning that these methods' accuracy changes by parameters, which requires more modifications. From this study for the FRP RC deep beam date base, included in the present study, the following could be concluded:

1- The FRP RC deep beam is not covered by the codes ACI440-11-22 [10], or it is not covered very well by code CSA S806-12 [11].
2- The shear strength prediction of STM CSA S806-12 [11] is a conservative method that makes it uneconomical by using more quantities than required. Although it is conservative, it is the most appropriate and least distracting.
3- The models evaluated in this study are unsuitable for predicting the FRP RC deep beam shear strength. They are either unsafe or inaccurate.

4- The STM method considers the lowest stresses of struts, ties, or nodes. The node must be well supported to prevent local failure, reducing the shear strength capacity of deep beams.
5- The data on FRP-RC deep beams with web reinforcement were very limited. More studies are required to improve the shear strength prediction for FRP RC deep beams.
6- The studies investigating the fiber effect in FRP-RC deep beams are few.
7- Continual research and testing must be used to update and improve the models for predicting the shear strength of FRP-reinforced deep beams.

ACKNOWLEDGMENTS

The authors are grateful for the financial support towards this research by the Civil Engineering Department, College of Engineering, Mustansiriyah University. Postgraduate Research Accept No. 1914/16/6/2020. The authors would like to express their appreciation to the Tikrit Journal of Engineering Sciences staff and the valuable comments from the Reviewers.

REFERENCES

[1] ACI Committee 318, **Building Code Requirements for Structural Concrete (ACI 318-19) and Commentary (ACI 318R-19)**, American Concrete Institute, Farmington Hills, MI, 2019.
[2] El-Sayed AK, Shuraim AB. **Size Effect on Shear Resistance of High Strength Concrete Deep Beams**. *Materials and Structures* 2016; **49**(5): 1871-1882.
[3] Nawy EG. **Reinforced Concrete: A Fundamental Approach**. 2nd ed., Boca Raton: CRC Press; 2008.
[4] Ebrahim AE, Elmeligy OM, El-Metwally SE, Ghoneim MA, Askar HS. **Refined Strength Prediction of Concrete 2D Bottle-Shaped Struts**. *Journal of Structural Engineering* 2021; **4**(2):111-125.
[5] Bairán JM, Menduiña R, Marí A, Cladera A. **Shear Strength of Non-Slender Reinforced Concrete Beams**. *ACI Structural Journal* 2020; **117** (2): 277-289.
[6] Kong FK. **Reinforced Concrete Deep Beams**. 1st ed., London: Blackie and Son Ltd.; 1991.
[7] El Zareef MA, Elbisy MS, Badawi M. **Evaluation of Code Provisions Predicting, the Concrete Shear Strength of FRP-Reinforced Members without Shear Reinforcement**. *Composite Structures* 2021; **275**: 114430.
[8] Chen H, Yi WJ, Ma ZJ, Hwang HJ. **Modeling of Shear Mechanisms and Strength of Concrete Deep Beams Reinforced with FRP Bars**. *Composite Structures* 2020; **234**: 111715.
[9] ACI Committee. ACI 440.1R-15: Guide for The Design and Construction of Structural Concrete Reinforced with FRP Bars. American Concrete Institute, Farmington Hills, 2015.
[10] ACI Committee 440. Building Code Requirements for Structural Concrete Reinforced with Glass Fiber-Reinforced Polymer (GFRP) Bars-Code and Commentary. ACI 440.11.22. American Concrete Institute, Farmington Hills, MI, 2022.
[11] CSA Standard S806-12. Design and Construction of Building Components with Fiber-Reinforced Polymers. (CSA) Canadian Standards Association, 2012.
[12] CSA Standard - A23.3-19: Design of Concrete Structures Canadian Standards Association. (CSA) Canadian Standards Association, 2019.
[13] Latosh FA. Structural Behaviour of Conventional and FRP-Reinforced Concrete Deep Beams. PhD Thesis. Concordia University; Montréal, Québec, Canada: 2014.
[14] Said M, Adam MA, Shanour AS. **Experimental and Analytical Shear Evaluation of Concrete Beams Reinforced with Glass Fiber Reinforced Polymers Bars**. *Construction and Building Materials* 2016; **102**: 574-591.
[15] Mohamed K, Farghaly AS, Benmokrane B. **Effect of Vertical and Horizontal Web Reinforcement on the Strength and Deformation of Concrete Deep Beams Reinforced with GFRP Bars**. *Journal of Structural Engineering* 2017; **143** (8): 04017079.
[16] Nassif MK, Erfan AM, Fadel OT, El-sayed TA. **Flexural Behavior of High Strength Concrete Deep Beams Reinforced with GFRP Bars**. *Case Studies in Construction Materials* 2021; **15**: e00613.
[17] El-Sayed AK, El-Salakawy EF, Benmokrane B. **Shear Strength of Fiber-Reinforced Polymer Reinforced Concrete Deep Beams Without Web Reinforcement**. *Canadian Journal of Civil Engineering* 2012; **39**(5): 546–555.
[18] Farghaly AS, Benmokrane B. **Shear Behavior of FRP-Reinforced Concrete Deep Beams without Web Reinforcement**. *Journal of Composite for Construction* 2013; **17** (6): 04013015.
[19] Abed F, El-Chabib H, AlHamaydeh M. **Shear Characteristics of GFRP-Reinforced Concrete Deep Beams**

Without Web Reinforcement. *Journal of Reinforced Plastics and Composites* 2012; **31**(16): 1063-1073.

[20] Kim DJ, Lee J, Lee YH. **Effectiveness Factor of Strut-and-Tie Model for Concrete Deep Beams Reinforced with FRP Rebars**. *Composites Part B: Engineering* 2014; **56**: 117-125.

[21] Andermatt MF, Lubell AS. **Behavior of Concrete Deep Beams Reinforced with Internal Fiber-Reinforced Polymer-Experimental Study**. *ACI Structural Journal* 2013; **110** (4): 585-594.

[22] Bediwy A, Mahmoud K, El-Salakawy E. **Structural Behavior of FRCC Layered Deep Beams Reinforced with GFRP Headed-End Bars**. *Engineering Structures* 2021; **243**: 112648.

[23] Hosseini SA, Nematzadeh M, Chastre C. **Prediction of Shear Behavior of Steel Fiber-Reinforced Rubberized Concrete Beams Reinforced with Glass Fiber-Reinforced Polymer (GFRP) Bars**. *Composite Structures* 2021; **256**: 113010.

[24] Thomas J, Ramadass S. **Improved Empirical Model for the Strut Efficiency Factor and the Stiffness Degradation Coefficient for the Strength and the Deflection Prediction of FRP RC Deep Beams**. *Structures* 2021; **29**: 2044-2066.

[25] Liu HX, Yang JW, Wang XZ, Han DJ. **Experimental Study on Shear Behavior of BFRP-Reinforced Recycled Aggregate Concrete Deep Beams without Stirrups**. *KSCE Journal of Civil Engineering* 2017; **21**(6): 2289-2299.

[26] Alhamad S, Al Banna Y, Al Osman A, Mouthassseeb J, Abdalla S, Abed F. **Effect of Shear Span-to-Depth ratio on the Shear Behavior of BFRP-RC Deep Beams**. *MATEC Web of Conferences* 2017; **120**: 01012, (1-7).

[27] Abed F, Sabbagh MK, Karzad AS. **Effect of Basalt Microfibers on the Shear Response of Short Concrete Beams Reinforced with BFRP Bars**. *Composite Structures* 2021; **269**: 114029.

[28] Darwin D, Dolan CW, Nilson AH. **Design of Concrete Structures**. 15th ed., New York, USA: McGraw-Hill Education; 2016.

[29] ACI Committee 445. **Strut-and-Tie Method Guidelines for ACI 318-19-Guide**. ACI-ASCE Committee PRC-445.2-21. (ACI) American Concrete Institute, 2021.

[30] Schlaich J, Schafer K. **Design and Detailing of Structural Concrete Using Strut-and-Tie Models**. *Structural Engineering* 1991; **69**(6): 113-125.

[31] Zhang T, Oehlers DJ, Visintin P. **Shear Strength of FRP RC Beams and One-Way Slabs without Stirrups**. *Journal of Composites for Construction* 2014; **18** (5): 04014007.

[32] Nehdi M, El Chabib H, Saïd AA. **Proposed Shear Design Equations for FRP-Reinforced Concrete Beams Based on Genetic Algorithms Approach**. *Journal of Materials in Civil Engineering* 2007; **19** (12): 1033-1042.

[33] Wight JK, McGregor JG. **Reinforced Concrete Mechanics and Design**. 7th ed. New Jersey: Person; 2012.

[34] Tan KH, Cheng GH. **Size Effect on Shear Strength of Deep Beams: Investigating with Strut-and-Tie Model**. *Journal of Structural Engineering* 2006; **132** (5): 673-685.